

An application of Galactic parallax: the distance to the tidal stream GD-1

Andy Eyre

Rudolf Peierls Centre for Theoretical Physics, Keble Road, Oxford OX1 3NP, UK

17 October 2009

ABSTRACT

We assess the practicality of computing the distance to stellar streams in our Galaxy, using the method of Galactic parallax suggested by Eyre & Binney (2009). We find that the uncertainty in Galactic parallax is dependent upon the specific geometry of the problem in question. In the case of the tidal stream GD-1, the problem geometry indicates that available proper motion data, with individual accuracy $\sim 4 \text{ mas yr}^{-1}$, should allow estimation of its distance with about 50 percent uncertainty. Proper motions accurate to $\sim 1 \text{ mas yr}^{-1}$, which are expected from the forthcoming Pan-STARRS PS-1 survey, will allow estimation of its distance to about 10 percent uncertainty. Proper motions from the future LSST and Gaia projects will be more accurate still, and will allow the parallax for a stream 30 kpc distant to be measured with ~ 14 percent uncertainty.

We demonstrate the feasibility of the method and show that our uncertainty estimates are accurate by computing Galactic parallax using simulated data for the GD-1 stream. We also apply the method to actual data for the GD-1 stream, published by Koposov et al. (2009). With the exception of one datum, the distances estimated using Galactic parallax match photometric estimates with less than 1 kpc discrepancy. The scatter in the distances recovered using Galactic parallax is very low, suggesting that the proper motion uncertainty reported by Koposov et al. (2009) is in fact over-estimated.

We conclude that the GD-1 stream is (8 ± 1) kpc distant, on a retrograde orbit inclined 37° to the plane, and that the visible portion of the stream is likely to be near pericentre.

Key words: astrometry – methods: numerical – methods: data analysis – Galaxy: structure

1 INTRODUCTION

Measuring distances in our Galaxy is critical to understanding its structure. However, line-of-sight distances can typically be measured with only relatively poor precision. This lack of precision is manifest in the most basic of Galactic parameters; the solar radius R_0 is hardly known to better than 5 percent uncertainty (Gillessen et al. 2009), and this result renders the circular velocity at R_0 similarly uncertain (McMillan & Binney 2009). An accurate knowledge of distances is essential to create convincing models of the Milky Way, which in turn influence our understanding of the physics of galaxy formation in general.

Conventional trigonometric parallax has long been used to calculate accurate distances to nearby stars. The regular nature of the parallactic motion of a star, caused by the Earth’s orbit around the Sun, allows this motion to be decoupled from the intrinsic proper motion of the star in the

heliocentric rest frame. Hence the distance to the star can be calculated. However, the maximum baseline generating such parallaxes is obviously limited to 2AU. For a given level of astrometric precision, this imposes a fundamental limit to the observable distance. Indeed, the accuracy of parallaxes reported by the Hipparcos mission data (van Leeuwen 2007) falls to 20–30 percent at best for distances ~ 300 pc and only then for the brightest stars. Upcoming astrometric projects such as Pan-STARRS (Kaiser et al. 2002), LSST (Tyson 2002) and the Gaia mission (Perryman et al. 2001) will achieve similar uncertainty for Sun-like stars as distant as a few kpc, and at fainter magnitudes than was possible with Hipparcos. This extended range will encompass less than 1 percent of the total number of such stars in our Galaxy.

It is clear that it will *not* soon be possible to calculate distances to many of the stars in our Galaxy with conven-

tional trigonometric parallaxes. Alternative means to compute distances to stars are therefore required. Photometry can be used to estimate the absolute magnitude of a star which, when combined with its observed magnitude, allows its distance to be computed. Unfortunately, all attempts to calculate such photometric distances are hindered by the same problems: obscuration by intervening matter alters both observed magnitude (Vergely et al. 1998) and colour (Schlegel et al. 1998; Drimmel & Spergel 2001), and it is difficult to model appropriate corrections without a reference distance scale. The effects of chemical composition and age further complicate matters (Jurić et al. 2008). It is therefore difficult to compute photometric distances with an accuracy much better than 20 percent, even for nearby stars, and distances to faint stars are less accurate still (Jurić et al. 2008).

Latterly, it was realised (Eyre & Binney 2009, hereafter Paper I) that the orbital motion of the Sun about the Galaxy could be used to compute trigonometric distances to stars. In the general case, it is not possible to do this because the parallactic motion of a star and its intrinsic proper motion are inextricably mixed up. However, in the special case where the star can be associated with a stellar stream, its rest-frame trajectory can be predicted from the locations of the other associated stars. Using this trajectory, the proper motion in the Galactic rest frame can indeed be decoupled from the reflex motion of the Sun, and the component of its motion due to parallax can be computed.

Such ‘Galactic parallaxes’ have the same geometrical basis as conventional trigonometric parallaxes, and as such are free from errors induced by obscuration and reddening. However, the range of Galactic parallax significantly exceeds that of conventional parallax. This is because the Sun orbits about the Galactic centre much faster than the Earth orbits the Sun, and because, unlike with conventional parallax, the Galactic parallax effect is cumulative with continued observation. In realistic cases, for a typically oriented stream, we can expect the Galactic parallax to be observable at nearly 40 times the distance of the equivalent trigonometric parallax, based on 3 years of observations. For increased range, one simply observes over a longer baseline.

This large range means that Galactic parallax might prove a powerful tool to complement conventional parallaxes, and validate other distance measuring tools. It is exciting to note that the capabilities of astrometric projects such as LSST, which will observe the conventional parallax of a G star at a distance of ~ 1 kpc with 20 percent uncertainty, will put much of the Galaxy in range of Galactic parallax calculations with similar accuracy.

The main restriction on the use of Galactic parallax is the requirement for stars to be part of a stream. However, the continuing discovery of significant numbers of streams (Odenkirchen et al. 2002; Majewski et al. 2003; Yanny et al. 2003; Belokurov et al. 2006; Grillmair 2006; Grillmair & Dionatos 2006; Grillmair & Johnson 2006; Grillmair 2009; Newberg, Yanny, & Willett 2009) using optical surveys implies that they are a staple feature of the Galactic environment, rather than a rarity. The deep surveys of Pan-STARRS and LSST are likely to find yet more, increasing the number of applications for Galactic parallax.

This paper explores the viability of using Galactic parallax to estimate distances and demonstrates its practicality by applying it to data for the GD-1 stream

(Grillmair & Dionatos 2006) published by Koposov et al. (2009, hereafter K09); we choose to work with the latter over the earlier analysis of the same stream by Willett et al. (2009) on account of the significantly smaller proper motion uncertainties (1 mas yr^{-1} vs 4 mas yr^{-1}) cited in the later work. Throughout this paper, the Solar motion is assumed to be $(U, V, W) = (10.0, 252, 7.1) \pm (0.3, 11, 0.34) \text{ km s}^{-1}$, consistent with Aumer & Binney (2009), Reid & Brunthaler (2004) and Gillessen et al. (2009).

The paper is arranged as follows. Section 2 reviews the calculation of Galactic parallax, and explores the uncertainty affecting such calculations, and how this uncertainty affects practical application. Section 3 demonstrates the viability of the method by applying it to pseudo-data, and Section 4 applies the method to actual data for the GD-1 stream. Section 5 summarizes our conclusions.

2 GALACTIC PARALLAX

Suppose that a star is part of a stellar stream, and has a location relative to the Sun described by $(\mathbf{x} - \mathbf{x}_0) = r\hat{\mathbf{r}}$, where r is the distance to the star, and \mathbf{x}_0 is the position of the Sun. In the plane of the sky, let the tangent to the trajectory of the stream, near the star, be indicated by the vector $\hat{\mathbf{p}}$. Assume the velocity of the Sun, \mathbf{v}_0 , in the Galactic rest frame (grf) is known. Paper I showed that if the measured proper motion of the star is $\mu\hat{\mathbf{t}}$, then

$$\dot{u}\hat{\mathbf{p}} = \mu\hat{\mathbf{t}} + \frac{\mathbf{v}_s}{r} = \mu\hat{\mathbf{t}} + \Pi\mathbf{v}_s, \quad (1)$$

where $\Pi \equiv 1/r$ is the Galactic parallax, \dot{u} is the proper motion as would be seen from the grf, and \mathbf{v}_s is the Sun’s velocity projected into the plane of the sky. We note that $\dot{u} = v_t/r$, where v_t is that component of the star’s grf velocity perpendicular to the line-of-sight, and that,

$$\mathbf{v}_s = (\mathbf{v}_0 - \hat{\mathbf{r}} \cdot \mathbf{v}_0 \hat{\mathbf{r}}). \quad (2)$$

Eq. 1 is a vector expression and can be solved simultaneously for both \dot{u} and Π provided that $\hat{\mathbf{p}}$, $\hat{\mathbf{t}}$ and \mathbf{v}_s are not parallel. The stream direction $\hat{\mathbf{p}}$ will not typically be known outright, but must be estimated from the positions of stream stars on the sky. We can achieve this by fitting a low order curve through the position data, the tangent of which is then taken to be $\hat{\mathbf{p}}$. The curve must be chosen to reproduce the gross behaviour of the stream, but we must avoid fitting high-frequency noise, because $\hat{\mathbf{p}}$ is a function of the derivative of this curve, which is sensitive to such noise.

2.1 Uncertainty in Galactic parallax calculations

We begin by rendering Eq. 1 into an orthogonal on-sky coordinate system, whose components are denoted by (x, y) . In this coordinate system Eq. 1 can be solved for Π ,

$$\Pi = \frac{\mu(t_x \sin \alpha - t_y \cos \alpha)}{v_{s,y} \cos \alpha - v_{s,x} \sin \alpha}, \quad (3)$$

where the (x, y) suffixes denote the corresponding components of their respective vectors, and where we have defined the angle $\alpha \equiv \arctan(p_y/p_x)$.

The choice of coordinates (x, y) is arbitrary. We are therefore free to choose the coordinate system in which

$\alpha = 0$, i.e. that system in which the x -axis points along the stream trajectory, $\hat{\mathbf{p}}$. Eq. 3 becomes,

$$\Pi = -\frac{\mu t_{\perp}}{v_{s\perp}}, \quad (4)$$

where we now identify the y -component of the various vectors as that component perpendicular (\perp) to the stream trajectory, and the x -component as that component parallel (\parallel) to the trajectory. Eq. 4 shows explicitly that the Galactic parallax effect is due to the reflex motion of stream stars perpendicular to the direction of their travel.

Uncertainties in the (x, y) components of the measured quantities $\mu\hat{\mathbf{t}}$ and \mathbf{v}_s , and uncertainty in α , can be propagated to Π using Eq. 3. When we set $\alpha = 0$, this equation becomes,

$$\frac{\sigma_{\Pi}^2}{\Pi^2} = \frac{\sigma_{\mu}^2}{\mu^2 t_{\perp}^2} + \frac{\sigma_{v_{s\perp}}^2}{v_{s\perp}^2} + \frac{\sigma_{\alpha}^2}{v_{s\perp}^2} \left(v_{s\parallel} + \frac{\mu t_{\parallel}}{\Pi} \right)^2, \quad (5)$$

where we anticipate the uncertainty in $\mu\hat{\mathbf{t}}$ to be isotropic, and so we have set $\sigma_{\mu t_x} = \sigma_{\mu t_y} = \sigma_{\mu}$.

We assume σ_{μ} to be known from observations; it may contain any combination of random and systematic error. $\sigma_{v_{s\perp}}$ is calculated directly from the error ellipsoid on \mathbf{v}_0 , which is assumed known. Any error on \mathbf{v}_0 affects all data in exactly the same way. However, the projection of error on \mathbf{v}_0 to \mathbf{v}_s varies with position on the sky. Hence, the effect of $\sigma_{\mathbf{v}_s}$ is to produce a systematic error in reported distance that varies along the stream in a problem-specific way.

Uncertainty in α arises from two sources. Firstly, because the on-sky trajectory $\hat{\mathbf{p}}$ is chosen by fitting a smooth curve through observational fields, $\hat{\mathbf{p}}$ need not be exactly parallel to the underlying stream. Further, since $\hat{\mathbf{p}}$ depends on the derivative of the fitted curve, it is likely to be much less well constrained for the data points at the ends of the stream than for those near the middle.

We can quantify this effect. At the endpoints, the fitted curve is likely to depart from the stream by at most $\Delta\psi$, the angular width of the stream on the sky. For a low-order curve, this departure is likely to have been gradual over approximately half the angular stream length, $\Delta\theta$, giving a contribution to σ_{α} from fitting of,

$$\sigma_{\alpha,f}^2 = \frac{4\Delta\psi^2}{\Delta\theta^2}. \quad (6)$$

The second contribution to σ_{α} arises as follows. Since the stream has finite width, at any point, the stars within it have a spread of velocities, corresponding to the spread in action of the orbits that make up the stream. If the stars in a stream show a spread in velocity ($\sigma_{v_x}, \sigma_{v_y}$) about a mean velocity $\mathbf{v}_t = r\dot{\mathbf{u}}\hat{\mathbf{p}}$, this effect contributes,

$$\sigma_{\alpha,v}^2 = \frac{1}{v_t^2} (\sigma_{v_y}^2 \cos^2 \alpha + \sigma_{v_x}^2 \sin^2 \alpha), \quad (7)$$

to the uncertainty in α for a single star. Again we can choose $\alpha = 0$, such that $\sigma_{v_y} = \sigma_{v\perp}$, the velocity dispersion perpendicular to the stream direction. Eq. 7 becomes,

$$\sigma_{\alpha,v}^2 = \frac{\sigma_{v\perp}^2}{v_t^2} = \frac{\sigma_{v\perp}^2}{(v \sin \beta)^2}, \quad (8)$$

where we have introduced v , the grf speed of the stream, and β , the angle of the stream to the line-of-sight. $\sigma_{v\perp}$ has its origin in the random motions of stars that existed within the progenitor object. In fact, if we assume the stream has

not spread significantly in width, then the width and the velocity dispersion (Binney & Tremaine 2008, §8.3.3) are approximately related by,

$$\frac{\sigma_{v\perp}}{v} \simeq \frac{w}{R_p} = \frac{r\Delta\psi}{R_p}, \quad (9)$$

where w is the physical width of the stream, and R_p is the radius of the stream's perigalacticon. This gives,

$$\sigma_{\alpha,v} = \frac{r\Delta\psi}{R_p \sin \beta}. \quad (10)$$

If secular spread has made the stream become wider over time, then this relation will over-estimate $\sigma_{\alpha,v}$, since $\sigma_{v\perp}/v$ is roughly constant. $\Delta\psi$ therefore represents an upper bound on the true value of $\sigma_{\alpha,v}$ through this relation. This argument also assumes that the stream was created from its progenitor in a single tidal event. Real streams do not form in this way. However, repeated tidal disruptions can be viewed as a superposition of ever younger streams, created from a progenitor of ever smaller $\sigma_{v\perp}$. Eq. 10 holds for each of these individually. Thus, $\Delta\psi$ remains a good upper bound for $\sigma_{\alpha,v}$ through this relation.

In reality, we do not measure the proper motion of individual stream stars, but rather the mean motion of a field of N stars. The contribution to σ_{α} is from the error on this mean. Putting this together with Eq. 6 gives our final expression for σ_{α} ,

$$\sigma_{\alpha}^2 = \frac{\sigma_{\alpha,v}^2}{N} + \sigma_{\alpha,f}^2 = \frac{r^2 \Delta\psi^2}{NR_p^2 \sin^2 \beta} + \frac{4\Delta\psi}{\Delta\theta^2}. \quad (11)$$

We note that the first term represents a random error, and the second term represents a systematic error that will vary with position down the stream. In general, $\sin \beta$ and R_p are a priori unknown. We can infer $\sin \beta$ from radial velocity information, either directly where the measurements exist, or indirectly from Galactic parallax distances. Guessing R_p requires assumptions to be made about the dynamics, but in general we expect the ratio $r/R_p \simeq 1$ or less.

Explicit evaluation of $\sin \beta$ and R_p are not necessary to evaluate the uncertainty if σ_{α} is dominated by the error from fitting, $\sigma_{\alpha,f}$. We can see this will be the case when the number of observed stars per field,

$$N > \left(\frac{r\Delta\theta}{2R_p \sin \beta} \right)^2. \quad (12)$$

We expect this to be true in almost all practical cases.

2.2 Uncertainty in tangential velocity calculations

Eq. 1 can also be used to solve for \dot{u} ,

$$\dot{u} = \frac{\mu(t_y + t_x) + \Pi(v_{s,y} + v_{s,x})}{\cos \alpha + \sin \alpha}, \quad (13)$$

which becomes,

$$\dot{u} = \mu(t_{\parallel} + t_{\perp}) + \Pi(v_{s\parallel} + v_{s\perp}) = \mu t_{\parallel} + \Pi v_{s\parallel}, \quad (14)$$

when we set $\alpha = 0$. Eq. 13 combined with Eq. 3 can be used to explicitly propagate uncertainties in the measured quantities to \dot{u} . When $\alpha = 0$, the uncertainty in \dot{u} is,

$$\frac{\sigma_{\dot{u}}^2}{\dot{u}^2} = \frac{\mathbf{v}_s^2 \sigma_{\mu}^2}{\mu^2 (t_{\perp} v_{s\parallel} - t_{\parallel} v_{s\perp})^2} + \frac{t_{\perp}^2 (v_{s\perp}^2 \sigma_{v_{s\parallel}}^2 + v_{s\parallel}^2 \sigma_{v_{s\perp}}^2)}{v_{s\perp}^2 (t_{\perp} v_{s\parallel} - t_{\parallel} v_{s\perp})^2}$$

$$- \frac{2t_{\perp}^2 v_{s\parallel} v_{s\perp} \text{cov}(v_{s\parallel}, v_{s\perp})}{v_{s\perp}^2 (t_{\perp} v_{s\parallel} - t_{\parallel} v_{s\perp})^2} + \frac{v_{s\parallel}^2 \sigma_{\alpha}^2}{v_{s\perp}^2}. \quad (15)$$

$\sigma_{v_{s\parallel}}$ and $\text{cov}(v_{s\parallel}, v_{s\perp})$ are calculated directly from the error ellipsoid on \mathbf{v}_0 , which we have assumed known.

2.3 Practicality of Galactic parallax as a distance measuring tool

Using Eq. 4 to eliminate μt_{\perp} from Eq. 5, and taking the dot product of $\hat{\mathbf{p}}$ with Eq. 1 to simplify the last term, we obtain,

$$\begin{aligned} \frac{\sigma_{\Pi}^2}{\Pi^2} &= \frac{1}{v_{s\perp}^2} \left\{ (r\sigma_{\mu})^2 + \sigma_{v_{s\perp}}^2 + (r\dot{u})^2 \sigma_{\alpha}^2 \right\} \\ &= \frac{1}{v_{s\perp}^2} \left\{ (r\sigma_{\mu})^2 + \sigma_{v_{s\perp}}^2 + v^2 \left(\frac{r^2 \Delta\psi^2}{R_p^2 N} + \frac{4\Delta\psi^2}{\Delta\Theta^2} \right) \right\}, \quad (16) \end{aligned}$$

where we have noted that $r\dot{u} = v_t = v \sin \beta$, and we have related the observed stream length, $\Delta\theta$, to the deprojected length, $\Delta\theta = \Delta\Theta \sin \beta$. We note that the last term is independent of r , since $r\Delta\psi = w$ and $\Delta\psi/\Delta\Theta$ are both constant, and that for a stream of given physical dimension, the uncertainty in Π has no dependence upon the angle of the stream β to the line of sight.

What level of uncertainty does Eq. 16 predict, when realistic measurement errors are introduced? The answer to this is dependent upon the both the physical properties of the stream ($R_p, \Delta\psi, \Delta\Theta, v$) and the geometry of the problem in question ($r, v_{s\perp}$).

We progress by assuming ‘typical’ values for some of these quantities. The average magnitude of \mathbf{v}_s taken over the whole sky is $v_0 \pi/4$. The average perpendicular component, for a randomly oriented stream, is $2/\pi$ of this value. We therefore assume a typical value for $v_{s\perp}$ of $v_0/2 \sim 120 \text{ km s}^{-1}$. We also assume a typical grf velocity equal to the circular velocity, $v = v_c \sim 220 \text{ km s}^{-1}$.

McMillan & Binney (2009) recently summarised the current state of knowledge of \mathbf{v}_0 . The uncertainty quoted is typically ~ 5 percent on each of (U, V, W). Correspondingly, we estimate a typical value for the uncertainty $\sigma_{v_{s\perp}}$ of 5 percent of $v_{s\perp}$, or 6 km s^{-1} .

The GD-1 stream that we consider below is exceptionally thin and long, with $\Delta\psi \sim 0.1^\circ$ and $\Delta\theta \sim 60^\circ$. The Orphan stream (Grillmair 2006; Belokurov et al. 2007) is of similar length, but about 10 times thicker. Both of these streams are near apsis, so $\Delta\theta = \Delta\Theta$. We therefore take $\Delta\psi \sim 1^\circ$, $\Delta\Theta \sim 60^\circ$ as typical of the streams to which one would apply this method. If hundreds of stars are observed for each proper motion datum, then Eq. 12 is true for all realistic combinations of (r, R_p), so we can ignore the contribution of $\sigma_{\alpha, v}$ to σ_{α} . The contribution from $\sigma_{\alpha, f}$ gives $\sigma_{\alpha} \simeq 1.9^\circ$.

The individual USNO/SDSS proper motions (Munn et al. 2004) used by K09 have a random uncertainty $\sigma_{\mu} \sim 4 \text{ mas yr}^{-1}$. After averaging over hundreds of stars and accounting for a contribution from non-stream stars, K09 report a random uncertainty of $\sigma_{\mu} \sim 1 \text{ mas yr}^{-1}$ on their GD-1 data. For a stream 10 kpc distant, with these proper motions and the typical values mentioned, Eq. 16 reports an uncertainty of $\sigma_{\Pi}/\Pi \sim 40$ percent. By far the greatest contribution comes from the first term in Eq. 16, hence, the error on proper motion measurement is dominating our uncertainty.

To obtain an uncertainty of $\sigma_{\Pi}/\Pi < 20$ percent with Munn et al. (2004) proper motion measurements, we would need to restrict ourselves to streams less than 5 kpc distant. 20 percent error is also possible at 10 kpc given optimum problem geometry. This is clearly competitive with the ~ 20 pc at which one could observe a standard trigonometric parallax, with similar accuracy, using astrometry of this quality. However, previous work (Willett et al. 2009, K09) shows that SDSS photometry combined with population models produce distance estimates accurate to ~ 10 percent for stars in streams at 8 kpc. The accuracy of Galactic parallax is therefore not likely to be as good as that of photometric distances for distant streams, using data this poor, unless the problem geometry is favourable.

Proper-motion data from the Pan-STARRS telescope is expected to be accurate to $\sim 1 \text{ mas yr}^{-1}$ for Sun-like stars at 10 kpc (Magnier et al. 2008). K09 reduce raw data with accuracy $\sim 4 \text{ mas yr}^{-1}$ to processed data accurate to $\sim 1 \text{ mas yr}^{-1}$, even though the expected proper motion of the stars is of the same size as the errors. It is not unreasonable to expect a similar analysis applied to Pan-STARRS raw data, where the relative error would be much less than unity, to yield processed data accurate to $\sim 0.2 \text{ mas yr}^{-1}$. In truth, the ability of Pan-STARRS to detect very faint stars will increase the number of stars identifiable with a stream, and thus reduce the uncertainty in the mean proper motion further than this, but we use 0.2 mas yr^{-1} as a conservative estimate.

The same 10 kpc distant stream would have a parallax error of $\sigma_{\Pi}/\Pi \simeq 11$ percent with data this accurate. An error of less than 20 percent is possible for a typical stream less than ~ 23 kpc distant, and for a stream with favourable geometry less than 50 kpc distant. Jurić et al. (2008) report that SDSS photometric distances for dwarf stars have ~ 40 percent error at 20 kpc. Thus, the accuracy of Galactic parallax derived from Pan-STARRS data should be at least comparable to distance estimates from photometric methods, even in the typical case.

Future projects such as LSST and Gaia will each obtain proper motions accurate to $\sim 0.2 \text{ mas yr}^{-1}$ for Sun-like stars 10 kpc distant (Ivezić et al. 2007; Perryman et al. 2001). These data would allow a distance estimate for our typical stream accurate to 8 percent, and a stream with favourable geometry accurate to 4 percent. Error in the proper motion no longer dominates the uncertainty in these calculations. We might expect such accurate astrometric surveys to reduce the uncertainty in the Solar motion; in this case, the error in parallax would be lower still.

Gaia will not observe Sun-like stars beyond 10 kpc, but LSST will, with accuracy of 0.4 mas yr^{-1} for dwarf stars 30 kpc distant (Ivezić et al. 2007). The accuracy of the parallax to our typical stream at this distance would be about 14 percent with these data, and 6 percent is achievable with optimum geometry. A typical stream could be measured to 20 percent accuracy out to 40 kpc, and a stream with favourable geometry out to 54 kpc; this range approaches the limit of LSST’s capability for detection of dwarf stars. Such data will put the Orphan stream, which is about 20 – 30 kpc distant (Grillmair 2006; Belokurov et al. 2007; Sales et al. 2008), in range of accurate trigonometric distance estimation. For comparison, photometric distances from SDSS data

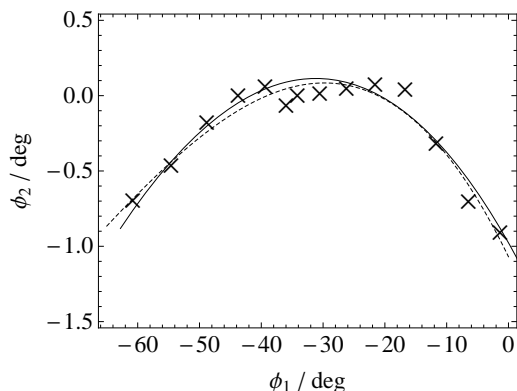


Figure 1. Full line: the orbit for the GD-1 stream, taken from K09. Crosses: pseudo-data derived from that orbit, but randomly scattered in ϕ_2 according to a Gaussian distribution with a dispersion of $\sigma_{\phi_2} = 0.1^\circ$. Dotted line: a cubic polynomial fitted to the pseudo-data, used to estimate stream direction.

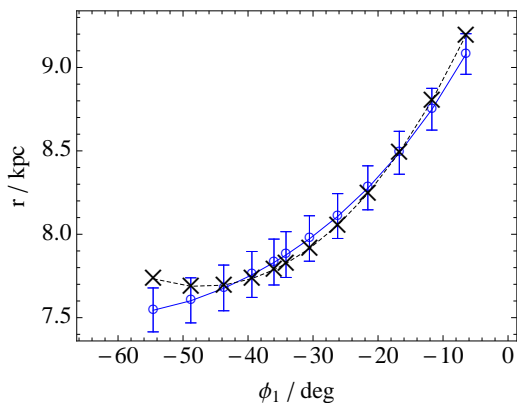


Figure 2. Dotted line: the orbit of the GD-1 stream, taken from K09. Crosses: the true distance of each pseudo-datum. Circles: Galactic parallax distances computed from the pseudo-data. The error bars represent the distance error expected from the polynomial fitting procedure. No extraneous error was added. The estimated errors are shown to be a good estimate of likely error from the fitting procedure, and the agreement of the distances overall is excellent.

are hardly more accurate than 50 percent for this stream (Belokurov et al. 2007).

3 TESTS

To test the method, pseudo-data was prepared from an orbit fitted to data for the GD-1 stream by K09. The orbit is described by the initial conditions $\mathbf{x} = (-3.41, 13.00, 9.58)$ kpc, $\mathbf{v} = (-200.4, -162.6, 13.9)$ km s $^{-1}$, where the x -axis points towards the Galactic centre, and the y -axis points in the direction of Galactic rotation. The orbit was integrated in the logarithmic potential,

$$\Phi(x, y, z) = \frac{v_c^2}{2} \log \left(x^2 + y^2 + \left(\frac{z}{q} \right)^2 \right), \quad (17)$$

where $v_c = 220$ km s $^{-1}$ and $q = 0.9$. The resulting trajectory was projected onto the sky, assuming a Solar radius

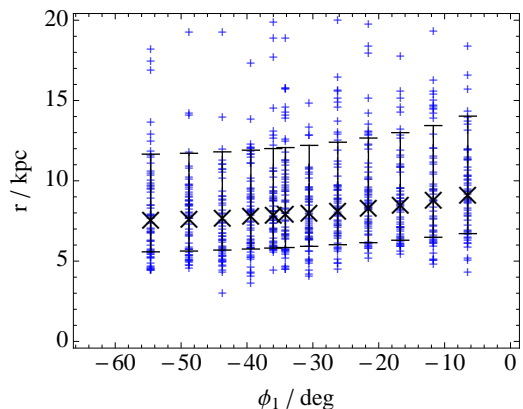


Figure 3. Crosses: Galactic parallax distances computed from the pseudo-data, with no extraneous errors. Error bars: the random scatter expected in Galactic parallax distances, with measurement errors as mentioned in the text. Plus signs: Galactic parallax distances computed from 60 Monte Carlo realisations of each pseudo-datum convolved with the measurement errors. The analytic uncertainty estimate and the Monte Carlo realisations are in good agreement.

$R_0 = 8.5$ kpc. Several points were sampled, and each was taken to be a separate datum in the pseudo-data set. The proper motion for each datum was computed by projecting the difference between its galactic motion and the Solar motion on to the sky.

The pseudo-data were transformed into the rotated coordinate system used by K09 to facilitate comparison with their data; the transformation rule is given in the appendix to K09. The stream is very flat in this coordinate system, so the dependence of ϕ_2 on ϕ_1 is relatively weak. This helps to increase the quality of the fitted curve and minimises the corresponding error in $\sigma_{\alpha, f}$.

To simulate the observed scatter in the real positional data, the pseudo-data were each scattered in the ϕ_2 coordinate according to a randomly-sampled Gaussian distribution with a dispersion $\sigma_{\phi_2} = 0.1^\circ$. The resulting positional pseudo-data are plotted in Fig. 1, along with the orbit from which they were derived (full curve). A cubic polynomial representing $\phi_2(\phi_1)$ was least-squares fitted to the pseudo-data, the tangent of which was used to estimate $\hat{\mathbf{p}}$. In the case of the pseudo-data, uniform weights were applied to each datum for the fitting processes. The resulting curve is also shown in Fig. 1 (dotted curve).

When the correct orbit is used to calculate $\hat{\mathbf{p}}$, and precise values for the measured proper motion $\mu \hat{\mathbf{t}}$ and Solar reflex motion \mathbf{v}_s are used, the distance is recovered perfectly from Eq. 4. Fig. 2 compares the recovered distance when $\hat{\mathbf{p}}$ is estimated using the polynomial fit to the pseudo-data, but still using accurate values for $\mu \hat{\mathbf{t}}$ and \mathbf{v}_s . Our pseudo-data stream is $\Delta\psi \simeq 0.1^\circ$ wide and $\Delta\theta \simeq 60^\circ$ long. Eq. 6 therefore estimates $\sigma_{\alpha, f} \simeq 0.38^\circ$. The recovered distances in Fig. 2 are in error by only ~ 2 percent across most of the range, which is the approximate uncertainty predicted by Eq. 5 for this value of $\sigma_{\alpha, f}$. Thus, the estimation of $\hat{\mathbf{p}}$ from the observed stream is good, and contributes little error to the distance calculations.

The K09 observational data for the GD-1 stream, discussed below, have a similar uncertainty $\sigma_\alpha \sim 0.38^\circ$ due

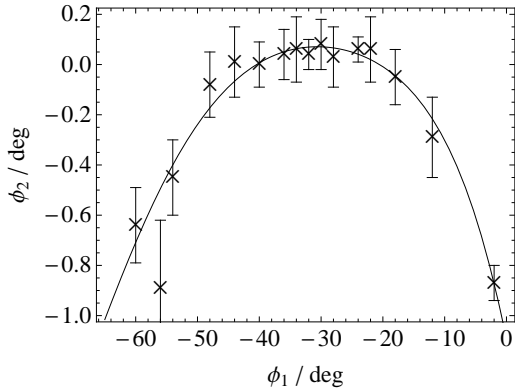


Figure 4. Crosses: on-sky position data for the GD-1 stream, as published in K09. The error bars represent the quoted uncertainties. Full line: linear least-squares fit of a cubic polynomial, $\phi_2(\phi_1)$, to these data; the inverse-square of the uncertainties was used to weight the fit.

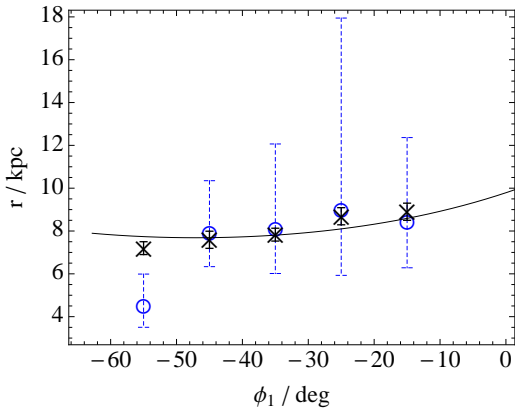


Figure 5. Circles: Galactic parallax distances for the GD-1 data presented in K09. Dotted error bars: the uncertainty estimated by Eq. 5, given the K09 measurement uncertainties. Crosses: the photometric distances reported in K09, along with their error bars. Full line: the orbit for GD-1 taken from K09. With the exception of the datum at $\phi_1 \sim -55$ deg, the Galactic parallax distances are in excellent agreement with the photometric distances from K09. The dotted error bars appear to seriously over-estimate the true error in the distance estimates.

entirely to the fitting process, and proper motion uncertainties $\sigma_\mu \sim 1 \text{ mas yr}^{-1}$. Fig. 3 shows the recovered distances from Fig. 2 with error bars for the expected uncertainty in recovered distance, given these measurement uncertainties and the uncertainty in \mathbf{v}_0 quoted in Section 1. Also plotted for each datum are the distances recovered from 60 Monte Carlo realisations of the pseudo-data input values, convolved with the errors given above.

Eq. 5 is found to be a good estimator for the uncertainty, with approximately 80 percent of the Monte Carlo realisations falling within the error bars. The error in parallax for the K09 data is thus predicted to be about 50 percent, of which the greatest contribution comes from the uncertainty in proper motion.

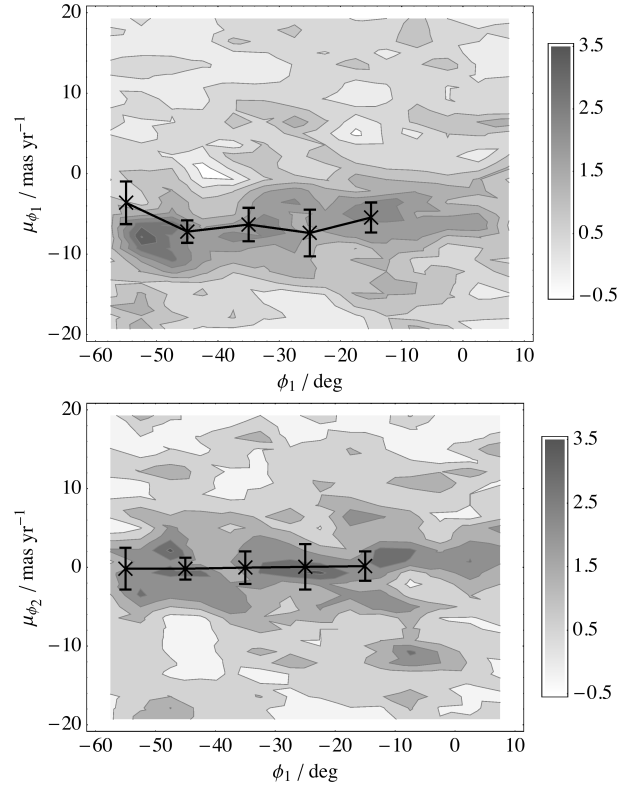


Figure 6. Full lines: Galactic-rest frame proper motion (\dot{u}) calculated from the K09 data using Eq. 14. The (upper, lower) panels show the (ϕ_1, ϕ_2) components respectively. Plotted in the background are the observational data from Fig. 9 in K09; the greyscale shows the number of stream stars, per bin, with the given motion. The data are broadly consistent, except for the datum at $\phi_1 \sim -55$ deg in the upper panel.

4 DISTANCE TO THE GD-1 STREAM

Fig. 4 shows the on-sky position data for the GD-1 stream, as published in K09. Also shown in Fig. 4 is a linear least-squares fit of a cubic polynomial to these data, used to estimate $\hat{\mathbf{p}}$. The weights for the fit were the inverse-square uncertainties for each position field, as given by K09.

K09 provide measured proper motion data for five fields of stars, spanning the range $\phi_1 \sim (-55, -15)^\circ$, along with uncertainties for these measurements. Uncertainty in the stream direction is $\sigma_\alpha \sim 0.38^\circ$, which is entirely contributed by the curve fit to the stream; since hundreds of stars contributed to the calculation of the proper motions, the contribution from the first term in Eq. 11 is negligible. The uncertainty in \mathbf{v}_s is computed for each individual field from the uncertainty in \mathbf{v}_0 given in Section 1.

Fig. 5 shows the Galactic parallax distances for each of these data, along with the K09 photometric distances. The dotted error bars represent the expected error in distance for the uncertainties given. The small solid error bars are the uncertainties reported by K09 for their photometric distances. The K09 orbit used to compute the earlier pseudo-data is plotted for comparison.

With the exception of the datum at $\phi_1 \sim -55^\circ$, the parallax distances and the K09 distances are in remarkable agreement. However, the dotted error bars vastly overestimate the true error in the results. If we ignore the datum

$\phi_1 \sim -55^\circ$, the scatter in the distance, $\sigma_r \sim 1$ kpc, is similar to that of the photometric distances, and consistent with a true random error of $\sigma_\mu \sim 0.3 \text{ mas yr}^{-1}$, and negligible systematic offset. We cannot explain this discrepancy, except by suggesting that the K09 proper motion measurements are more accurate than the published uncertainties suggest. This is corroborated by the top-right panel of Fig. 13 from K09 in which the μ_{ϕ_2} data, with the exception of the datum at $\phi_1 \sim -55^\circ$, show remarkably little scatter within their error bars.

Fig. 6 shows the Galactic rest-frame proper motions, \dot{u} , calculated from Eq. 14 along with their error bars, from Eq. 15. In the background are plotted the data from Fig. 9 of K09, which show the density of stars with a given grf proper motion in the sample of stars chosen to be candidate members of the stream, and after subtraction of a background field. The K09 grf proper motions have been calculated by correcting measured proper motion for the solar reflex motion, using an assumed distance of 8 kpc (Koposov, private communication); this assumption will cause a systematic error in the K09 proper motions, of order the distance error, which changes with position down the stream. The apparently large width of the stream in this plot is due to uncertainty in the underlying Munn et al. (2004) proper motion data.

The stream is clearly visible in this plot as the region of high density spanning $\phi_1 \sim (0, -60)^\circ$ with $\mu_{\phi_2} \simeq 0 \text{ mas yr}^{-1}$ and μ_{ϕ_1} falling slowly between $(-6, -10) \text{ mas yr}^{-1}$. Despite the expected systematic error, the estimates of \dot{u} from the parallax calculation are consistent with these data, with the exception of the same datum at $\phi_1 \sim -55^\circ$ that also reports an anomalous distance.

We explain this suspect datum as follows. From inspection of the top-right panel of Fig. 13 from K09, it is apparent that the μ_{ϕ_2} measurement for this datum is not in keeping with the trend. Conversely, the corresponding μ_{ϕ_1} measurement is not obviously in error. If the magnitude of μ_{ϕ_2} for this datum has been over-estimated by the K09 analysis, then Eq. 4 will over-estimate the parallax, and hence under-report the distance. Fig. 5 indicates that the distance for this datum is indeed under-reported.

The effect of such an error in μ_{ϕ_2} on the grf proper motion, \dot{u} , can be understood by considering Eq. 14. If Π is over-estimated, \dot{u} will be either over-estimated or under-estimated, depending on the relative sign of the two terms. In the case of GD-1, μt_{\parallel} and $v_{s\parallel}$ have opposite signs, so an over-estimated Π will result in an under-estimated \dot{u} . This too corresponds with the behaviour of the suspect datum in Fig. 6.

It is unknown why this particular datum should be significantly in error while the other data are not. There are no obvious structures in the lower panel of Fig. 6 which might cause the fitting algorithm in K09 to mistakenly return an incorrect value for μ_{ϕ_2} . Nonetheless, if the scatter in the other data are accepted as indicative of their true statistical error, it is clear that the datum at $\phi_1 \sim -55^\circ$ cannot represent the proper motions of GD-1 stars at that location. We therefore predict that an appropriate re-analysis of the proper-motion data, taking care to ensure that a signal from GD-1 stream stars is properly detected, will return a revised proper-motion of $\mu_{\phi_2} \sim -3 \text{ mas yr}^{-1}$.

In summary, it seems that Galactic parallax measure-

ments confirm the K09 photometric analysis, and predict that the stream is approximately (8 ± 1) kpc distant, where the uncertainty denotes the scatter in the results. Since Galactic parallax and photometric estimates are fundamentally independent, it seems unlikely that systematic errors in either would conspire to produce the same shift in distance; this implies that no systematic error is present.

We also calculate a grf proper motion for the stream of $\mu_{\phi_1} = (-7 \pm 2) \text{ mas yr}^{-1}$, corresponding to a grf tangential velocity of $(265 \pm 80) \text{ km s}^{-1}$ in a direction $(\mu_l \cos b, \mu_b) \simeq (0.8, -0.6)$. This implies that the stream is on a retrograde orbit, inclined to the Galactic plane by $\sim 37^\circ$, which is in accordance with previous results (Willett et al. 2009; Koposov et al. 2009).

The galactocentric radius of ~ 14.5 kpc does not seem to be changing rapidly along stream's length, which subtends $\sim 12^\circ$ when viewed from the Galactic centre. This implies that the observed stream is at an apsis. The grf velocity of the stream is faster than the circular velocity, $v_c \sim 220 \text{ km s}^{-1}$. This implies that the stream is at pericentre, although the large uncertainty prevents a firm conclusion from being drawn. We note that the radial velocity data in K09 would also imply that the stream is observed at pericentre.

5 CONCLUSIONS

We have demonstrated the practical application of a technique for computing Galactic parallax, as described by Paper I. This technique utilises the predictable trajectories of stars in a stream to identify the contribution of the reflex motion of the Sun to the observed proper motion. The parallax and the Galactic rest-frame proper motion follow from this.

The only assumption made is knowledge of the Galactic rest-frame velocity of the Sun. It is also a requirement that the observed stars are part of a stream. Recent evidence (Odenkirchen et al. 2002; Majewski et al. 2003; Yanny et al. 2003; Belokurov et al. 2006; Grillmair 2006; Grillmair & Dionatos 2006; Grillmair & Johnson 2006; Grillmair 2009; Newberg, Yanny, & Willett 2009) indicates that tidal streams are a common constituent of the Galactic halo, and so this technique should have widespread application.

We have derived an expression for the uncertainty in Galactic parallax calculations. We include contributions from measurement errors in proper motion and Solar motion, error in the estimation of stellar trajectories from the stream direction, and algorithmic error in the estimation of stream direction itself.

The uncertainty for calculations involving a particular stream is depend upon the size, location and orientation of the stream, as well as upon measurement errors. We estimate that using individual proper motions accurate to 4 mas yr^{-1} , available now in published surveys (Munn et al. 2004), the parallax of a 10 kpc distant stream with typical geometry could be measured with an uncertainty of 40 percent. The parallax of a stream with optimum geometry could be measured with approximately half this uncertainty.

Proper motion data from the forthcoming Pan-STARRS PS-1 survey (Kaiser et al. 2002; Magnier et al.

2008) will yield the distance to a typical 10 kpc distant stream with 11 percent accuracy, or the distance to a stream at 23 kpc with 20 percent accuracy; with favourable geometry this accuracy could be achieved for a stream as distant as 50 kpc. With data of this quality, the uncertainty in distances from Galactic parallaxes will be considerably lower than those of photometry for distant streams.

The LSST (Tyson 2002; Ivezić et al. 2007) and the Gaia mission (Perryman et al. 2001) will produce proper-motion data that are more accurate still. Such data would allow the distance to stars in a 10 kpc typical stream to be computed to an accuracy of order of 8 percent, where the limitation is now imposed by uncertainty in the solar motion and in the stream trajectory. It is likely that LSST and Gaia data will allow the uncertainty in the solar motion to be significantly reduced, so in reality much better precision can be expected at this distance. For streams 30 kpc distant, LSST proper motions will allow distance estimates as accurate as 14 percent to be made in the typical case, and 6 percent with optimum geometry. Thus, the high-quality astrometric data that is expected to be available in the next decade will allow parallax estimates for very distant streams to be made with unparalleled accuracy.

To test the method presented, we have created pseudodata simulating the GD-1 stream (Grillmair & Dionatos 2006). When the method is provided with error-free pseudodata, the correct parallax is computed perfectly. When errors are introduced into the pseudo-data, the reported parallax degrades in line with the uncertainty estimates.

We applied the method to the astrometric data for the GD-1 stream in Koposov et al. (2009). With the exception of a single datum, the Galactic parallax is remarkably consistent with the photometric distances quoted by Koposov et al. (2009). Indeed, the uncertainty in the measured proper motions quoted by Koposov et al. (2009) should produce significant error in the Galactic parallax. However, the scatter in the results is consistent a random error of only $\sim 0.3 \text{ mas yr}^{-1}$, and if the photometric distances of K09 are believed, no systematic offset. This is at odds with the typical uncertainty in the proper motion of $\sim 1 \text{ mas yr}^{-1}$ reported by Koposov et al. (2009). We cannot explain this discrepancy, other than to suggest that the Koposov et al. (2009) method for estimating error in the proper motions is producing significant over-estimates.

The Galactic rest-frame proper motions predicted for the stream are also consistent with observational data from Koposov et al. (2009), with the exception of the same datum that also reports an inconsistent distance. We conclude that the proper-motion associated with this datum is erroneous, and we predict that reanalysis of the stream stars near this datum will reveal a reduced proper-motion measurement of $\mu_{\phi_2} \sim 3 \text{ mas yr}^{-1}$.

Photometry and Galactic parallax produce fundamentally independent estimates of distance. The quality of the corroboration of the Koposov et al. (2009) photometric distance estimates for GD-1 by the Galactic parallax estimates presented here therefore lends weight to the conclusion that the predicted distance, in both cases, is correct. On this basis, we conclude that the GD-1 stream is about (8 ± 1) kpc distant from the Sun, on a retrograde orbit that is inclined 37° to the Galactic plane with a rest-frame velocity of

$(265 \pm 75) \text{ km s}^{-1}$. We also conclude that the visible portion of the stream is probably at pericentre.

The prospect of being able to map trigonometric distances in the Galaxy to high accuracy at tens of kiloparsecs range is indeed exciting. The distances generated using this method, although limited to stars in streams, could be used to calibrate other distance measuring tools, such as photometry, that would be more widely applicable. The technique is immediately applicable to any stream for which proper-motion data are currently available, although we anticipate limited accuracy until better proper-motion data are available.

Given enough parallax data points along a given stream, an orbit can be constructed by connecting those points. This orbit is predicted independently of any assumption about the Galactic potential, which it must strongly constrain. Constraints on the Galactic potential impose constraints on theories of galaxy formation and cosmology. It would seem that the combination of dynamics and Galaxy-scale precision astrometry, such as provided by this method, could well have profound implications for astrophysics in the future. At present, however, it is not obvious how to combine all sources of astrometric and dynamical information, to produce the tightest constraints on the potential. We therefore encourage the exploration of methods for combining this information, in anticipation of the arrival of higher quality astrometric data in the next few years.

ACKNOWLEDGMENTS

I thank Prof. James Binney for his insight and continued support during this work; and the Oxford Dynamics group for their helpful remarks. I also thank Prof. Andy Gould for his thoughts on uncertainties which provoked the analysis in section 2, Sergey Koposov for his provision of the data for Fig. 6, and the anonymous referee for his/her remarks. I acknowledge the support of PPARC/STFC during preparation of this work.

REFERENCES

- Aumer M., Binney J., 2009, MNRAS, 397, 1286
- Belokurov, V., et al., (15 authors) 2006b, ApJ, 642, L137
- Belokurov, V., et al., (22 authors) 2007, ApJ, 658, 337
- Binney J., Tremaine S., 2008, *Galactic Dynamics* 2nd ed., (Princeton: Princeton University Press)
- Drimmel R., Spergel D. N., 2001, ApJ, 556, 181
- Eyre A., Binney J., 2009, MNRAS, 399, L160 (Paper I)
- Gillessen S., Eisenhauer F., Trippe S., Alexander T., Genzel R., Martins F., Ott T., 2009, ApJ, 692, 1075
- Grillmair C. J., 2006, ApJ, 645, L37
- Grillmair C. J., Dionatos, O., 2006, ApJ, 643, L17
- Grillmair C. J., Johnson R., 2006, ApJ, 639, L17
- Grillmair C. J., 2009, ApJ, 693, 1118
- Ivezić Ž., et al., (12 authors) 2007, IAU Symposium, 248, 537
- Jurić M., et al., (26 authors) 2008, ApJ, 673, 864
- Kaiser N., et al., (26 authors) 2002, SPIE, 4836, 154
- Kennicutt R.C., et al., (25 authors) 1998, ApJ, 498, 181

- Koposov S.E., Rix H.-W., Hogg D.W., 2009, ApJ, in press (K09)
- van Leeuwen F., 2007, *Hipparcos, the New Reduction of the Raw Data*, (Springer)
- McMillan P.J., Binney J.J., MNRAS, submitted (arXiv:0907.4685)
- Majewski S. R., Skrutskie M. F., Weinberg M. D., Osthheimer J. C., 2003, ApJ, 599, 1082
- Magnier E.A., Liu M., Monet D.G., Chambers K.C., 2007, IAU Symposium, 248, 553
- Munn J. A., et al., (12 authors) 2004, AJ, 127, 3034
- Newberg H. J., Yanny B., Willett B. A., 2009, ApJ, 700, L61
- Odenkirchen M., Grebel E.V., Dehnen W., Rix H.-W., Cudworth K.M., 2002, AJ, 124, 1497
- Perryman, M.A.C., et al., (10 authors) 2001, A&A, 369, 329
- Reid M. J., 1993, ARA&A, 31, 345
- Reid M.J., Brunthaler A., 2004 ApJ 616, 872
- Romaniello M., et al., (9 authors) 2008, A&A, 488, 731
- Sales L. V., et al., (9 authors) 2008, MNRAS, 389, 1391
- Schlegel D. J., Finkbeiner D. P., Davis M., 1998, ApJ, 500, 525
- Tyson J.A., 2002, SPIE, 4836, 10
- Vergely J.-L., Ferrero R. F., Egret D., Koeppen J., 1998, A&A, 340, 543
- Willett B. A., Newberg H. J., Zhang H., Yanny B., Beers T. C., 2009, ApJ, 697, 207
- Yanny B., et al., 2003, ApJ, 588, 824